A gasoline fuel processor designed to study quick-start performance

S. Ahmed*, R. Ahluwalia, S.H.D. Lee, S. Lottes

Argonne National Laboratory, 9700 S. Cass Avenue, Argonne, IL 60439, USA

Abstract

A fast-start capability is a key requirement for on-board fuel processors for automotive fuel cell systems operating on gasoline fuel. This paper reports on the design and fabrication of a suitable fuel processor having this capability and discusses estimates of the start-up fuel consumption for the laboratory unit. Also discussed are the start-up strategy and the results of a start-up simulation, which showed that the fuel processor can deliver 90% of the rated hydrogen capacity in 60 s, producing a product gas that contains >30% hydrogen and <50 ppm carbon monoxide. The start-up fuel consumption was estimated on the basis of the thermal mass of the fabricated components; the 10-kW$_e$ laboratory unit was estimated to require >2.9 MJ of fuel energy.
© 2005 Elsevier B.V. All rights reserved.

Keywords: Fuel processor; Fast start; Reformer; Hydrogen; Gasoline; Automotive fuel cell

1. Introduction

On-board fuel processors (FPs) for automotive fuel cell systems have been studied for over a decade for the possible early introduction of fuel cell vehicles[1] into the automotive marketplace. These devices have the potential to eliminate the chicken-and-egg controversy – which comes first, the fuel cell car or the hydrogen refueling infrastructure – by allowing the use of a current infrastructure fuel such as gasoline. This approach would allow time to develop: (1) the hydrogen production and distribution infrastructure and (2) the technology to support the fast refueling and on-board hydrogen storage options capable of supporting a 300-mile driving range that automobile customers expect.

It has proved to be a major challenge to design a device capable of converting a complex hydrocarbon fuel such as gasoline into a hydrogen-rich reformate that could fuel a polymer-electrolyte fuel cell – with its extreme sensitivities to being poisoned by carbon monoxide, sulfur, ammonia, etc.,

– while also meeting all of the constraints and desirable features of the automotive platform (see Appendix A for the set of targets defined by the U.S. Department of Energy). Yet researchers and developers have responded to the challenge, demonstrating numerous new technologies (catalysts, reactor designs, membranes, heat exchangers, etc.) and setting new standards of performance (higher efficiency, compact and lightweight hardware, etc.) [1].

Despite the advances in efficiency, power density, etc., start-up performance has remained a concern. The shortest start-up time of 4 min [2] demonstrated by HydrogenSource LLC, while setting a new benchmark, is considerably longer than the 30–60 s start-up time sought by the automobile manufacturers. Furthermore, a significant amount of fuel energy is needed to heat the fuel processor to its operating temperature. This start-up fuel consumption would penalize the fuel economy of the fuel cell vehicle. To limit this penalty to an acceptable value, a start-up fuel energy consumption of 2 MJ (for a 50-kW$_e$ FP) was set as a target. The start-up energy requirement is discussed further in a later section of this paper.

This study was sponsored by the U.S. Department of Energy to generate data on fuel processor design, fabrication, operation and model development, to provide technical insight into the feasibility of on-board fuel processing. Led

---

* Corresponding author. Tel.: +1 630 252 4553; fax: +1 630 972 4553.
 E-mail address: ahmed@cmt.anl.gov (S. Ahmed).
[1] These vehicles include a battery to permit load leveling and regenerative braking.

by Argonne National Laboratory, the project (Feasibility of Acceptable Start Time Experimental Reformer—FASTER) was conducted by a consortium, with contributions from Los Alamos National Laboratory, Oak Ridge National Laboratory, Pacific Northwest National Laboratory, Precision Combustion Inc., ArvinMeritor and Quantum Group.

2. Objective and approach

The objective of the FASTER project was to study the feasibility of on-board fuel processing from the perspective of start-up performance in terms of: (1) the ability to deliver a significant fraction of the rated hydrogen capacity (in a reformate stream acceptable to a polymer electrolyte fuel cell) within 60 s and (2) limiting the fuel energy consumed to $40 \, kJ \, kW_e^{-1}$ (2 MJ for a 50-kW_e FP) or less, to heat the FP to its design point temperatures.

The approach was to design a fuel processor capable of a fast start, that is, design hardware and a start-up strategy that in combination could produce the requisite hydrogen flow rates within 60 s. The integrated FP consisted of an autothermal [3] reformer (ATR) followed by water–gas shift (WGS) and preferential oxidation (PrOx) reactors, which is a process strategy favored by many fuel cell system developers. The FP was designed to convert gasoline (low-sulfur, California reformulated gasoline) to deliver 90% of the rated hydrogen capacity in 60 s in a reformate stream that contains at least 30% hydrogen and less than 50 ppm carbon monoxide. The experimental hardware was fabricated to enable the collection of data, which served to validate computer models. These models were then used to project the performance of advanced FPs by considering alternative component designs and thermal integration strategies.

3. Fuel processor design

3.1. Start-up strategy

An on-board fuel processor should be designed to deliver sufficient hydrogen to the fuel cell stack such that the power available to the vehicle is not limited during the initial period of the drive cycle. In a fuel cell/battery hybrid vehicle, this translates to a tradeoff between the energy capacity of the battery (size, weight, cost, etc.) and the start-up performance of the fuel processor (time, fuel, etc.). In other words, the shorter the fuel processor start-up time, the smaller the battery pack that would be needed. It is possible to start the fuel processor by using electrical heating (requires adequate battery power and energy storage capacity), operating the vehicle with stored hydrogen, burning gasoline to rapidly heat the fuel processor or by utilizing some alternative energy source. However, practical solutions for the automotive application are limited by a myriad of factors, such as the amount of fuel needed at start up and its impact on the vehicle's fuel econ-
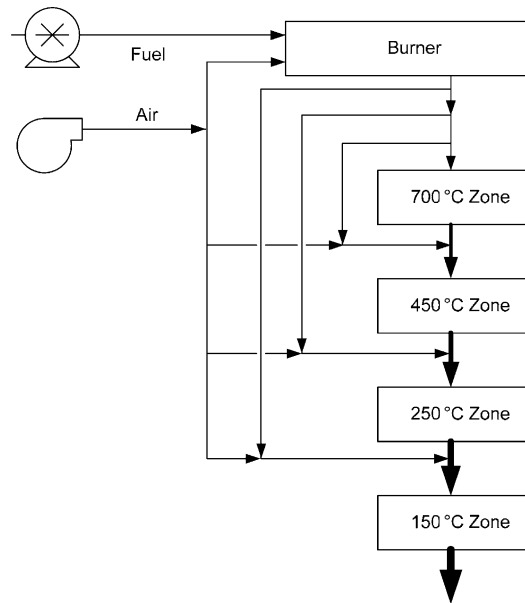

Fig. 1. Heating strategy using combustion air.

omy (miles per gallon), the need for equipment dedicated for start up, and the effects of thermal shock and cycling on durability, cost, etc. This difficult task is best approached by combining an effective design with a suitable start-up heating strategy.

With a generic ATR/WGS/PrOx-type fuel processor as a starting point, a number of start-up heating strategies were considered. We considered generating hot combustion gas in an external burner, and then injecting the hot gas at a temperature appropriate for the target zone (as shown in Fig. 1). This approach was rejected because it required an air handling capacity (dedicated blower) that was several times larger than would be needed during regular operation. Also, the components and conduits in the fuel processor would have to be significantly enlarged (increasing the FP mass and volume) to accommodate the large gas flows during start-up heating. Similarly, electrical heating was rejected, because in addition to the large battery necessary to store the requisite energy, the inefficient conversion of fuel to electrical energy would have imposed a large multiplier on the fuel consumed to provide the energy. For example, a fuel cell system net efficiency of 50% results in a multiplier of 2.

The implemented strategy consisted of taking advantage of the controllable exothermicity of the ATR. The essential features of the start-up strategy include the following elements:

- Using a small amount of electrical energy, ignite the fuel–air mixture on the reformer catalyst in the partial oxidation mode (no water), then switch to the autothermal mode by starting liquid water injection as the reforming catalyst warms up to a few hundred degrees. The reformer zone is thus able to rapidly produce a flammable gas mixture containing hydrogen and carbon monoxide.
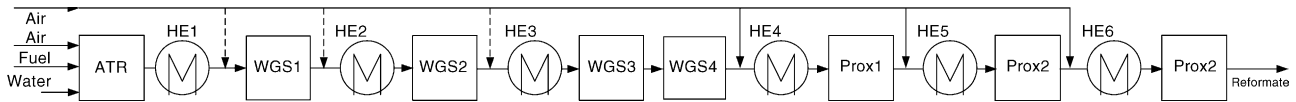
Fig. 2. Parallel heating strategy using reformate oxidation at WGS and PrOx zones.

- Use reactive heating in the essential zones with air injections to allow controlled oxidation of the flammable gases (H_2, CO) produced by the reformer. These essential zones include the water–gas shift reactor and the preferential oxidation zones [4,5]. Fig. 2 shows air injections upstream of the essential WGS and PrOx zones.

This start-up heating strategy offers several advantages. The parallel heating strategy (by simultaneous air injections) ensures simultaneous heating of the essential components. This approach also allows prioritization and eliminates delays in heating the downstream elements, as is typical in sequential heating. It additionally eliminates the need to flow large volumes of hot gas through the fuel processor and precludes the need to heat the heat exchangers, which are necessary for high fuel processing efficiency but not critical for reformate quality during the initial start up. In contrast, a sequential heating approach would delay the start up of downstream components or require very large mass flows of combustion gas.

3.2. The process train

Dynamic response, the ability to quickly change the processing rate, is an important feature of the on-board fuel processor, since it reduces the size of the battery needed to buffer the delay between when power is needed at the wheels and when hydrogen is available to the fuel cell to generate the power. Past experience has shown that catalytic reactors develop temperature profiles that depend on the processing rate. The readjustment of the temperature profile that accompanies changes in the processing rate can be quite significant (tens of degrees Celsius), takes time and affects product quality in the interim.

Automotive fuel processors are expected to go through numerous and often rapid changes in processing rate. Maintaining the inlet temperatures into each catalyst zone within a very narrow temperature band can eliminate the delay caused by the shifting of temperature profiles, and the fuel processor response is then only limited by the response times of the balance of the plant components that accommodate feed rate changes, i.e., the processor temperature profile does not change, only the air, fuel and water feed rates change with the changing hydrogen demand.

The WGS and PrOx catalyst zones are most effective (high conversion of desired reactions) when they can be operated at the design point. WGS and PrOx reactors are very sensitive to deviations from the design temperature because of selectivity and thermodynamic equilibrium; thus maintaining the design point temperature is critical to effective use of these components. To achieve this goal in the FASTER design, these reactors were separated by temperature-control
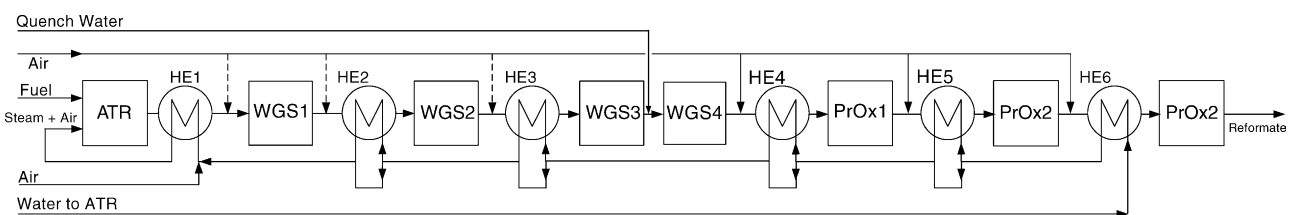

Fig. 3. Simplified schematic showing process streams in the fuel processor.

Table 1
Design conditions for the laboratory-scale (10-kW$_e$) fuel processor

	ATR	WGS1	WGS2	WGS3	WGS4	P1	P2	P3
GHSV ($K h^{-1}$)	74	66	41	22	13	37	37	37
Catalyst weight (kg)	0.15	0.24	0.38	0.69	1.15	0.29	0.29	0.29
Inlet temperature (°C)		375	350	300	280	140	140	100
Exit temperature (°C)	775	440	367	310	287	220	188	113
O/C ratio (at inlet)	0.75							
S/C ratio (at inlet)	2.1				2.3			
H_2 at exit (%-wet)	31.8	37.5	39.1	39.9	39.7	38.7	37.7	37.5
CO at exit (%-wet)	9.7	4.0	2.5	1.6	1.0	0.3	0.1	0.001
H_2O at exit (%-wet)	23.9	18.1	16.6	15.8	16.9	16.9	17.2	17.2
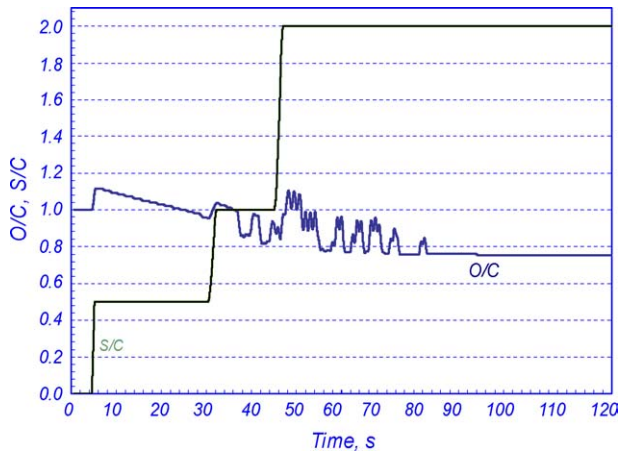
Fig. 4. Simulated feed conditions (oxygen-to-carbon and steam-to-carbon ratios) during the start-up period.

Fig. 5. Simulated temperature profiles in the ATR during start up.

zones—heat exchangers and liquid water injectors for cooling and air injectors for oxidative heating. Thus, the WGS and PrOx reactors were split into four and three stages, respectively. Fig. 3 is a simplified schematic showing the process streams within the fuel processor. Process water is the coolant in the heat exchangers. It flows counter-current to the direction of reformate flow, and its rate through the individual heat exchanger is controlled to maintain the set temperature for the reformate gas at that location. Thus, the fuel processing rate change is accompanied by corresponding changes in air and water rates and the temperature of the reformate gas entering each catalyst zone is maintained with the help of the coolant flow through the heat exchanger. The process water is converted into superheated steam within the six heat exchangers before entering the ATR. There is no heat exchanger between WGS3 and WGS4, and the cooling at that location is accomplished by injecting a small amount of water into the reformate stream.
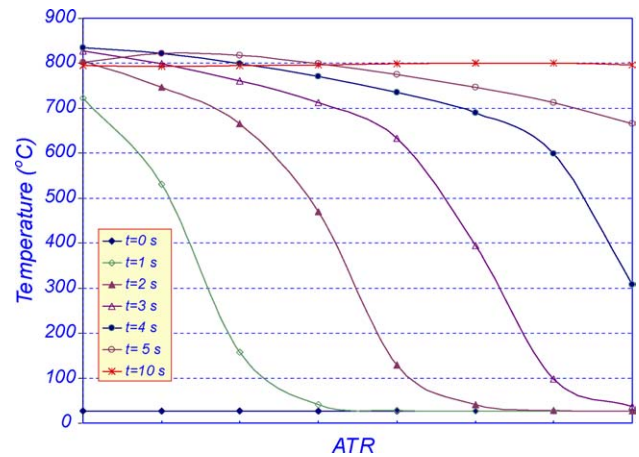
3.3. Design parameters

Table 1 lists the design conditions for the 10-kW$_e$ (40 g min^{-1} of gasoline) laboratory fuel processor, arrived at through numerous simulations and tradeoffs. At the converged steady-state design point, the fuel reacts with air at an oxygen-to-carbon atomic ratio (O/C) of 0.75 and with steam at a steam-to-carbon molar ratio (S/C) of 2.1. The product from the reformer exits at 775 °C, and is cooled in the first heat exchanger, HE1, to 375 °C before entering the first of four water–gas shift reactors. The gas hourly space velocity, the inlet and exit temperatures and the inlet/exit concentrations of hydrogen (H$_2$) and carbon monoxide (CO) are listed in the table. The reformate enters the PrOx zones containing 1% CO and emerges from the fuel processor with 0.001% (10 ppm) CO and 37.5% H$_2$ on a wet basis. The efficiency of the fuel processor, defined as the lower heating value (LHV) of hydrogen in the reformate as a
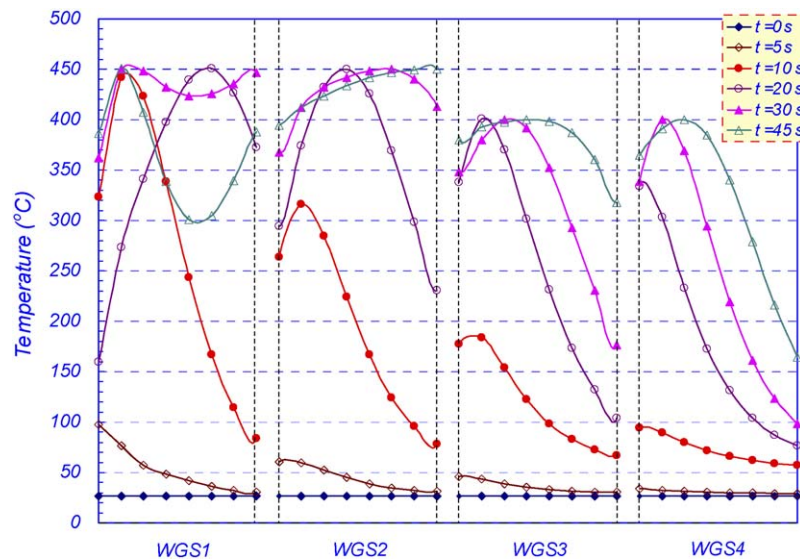

Fig. 6. Simulated temperature profiles in the four shift reactors during start up.
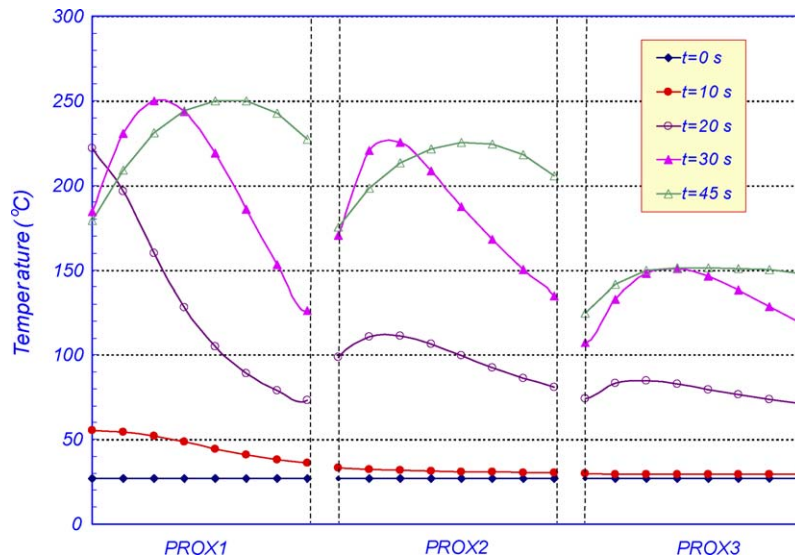
Fig. 7. Simulated temperature profiles in the three PrOx reactors during start up.

percentage of the LHV of the fuel feed, was calculated at 82%.

4. Simulating start up of the designed FP

A number of dynamic simulations were run to confirm that the apparatus as designed could be started up in 60 s. Figs. 4–7 present results from a simulation based on the use of a dual-function nozzle that can feed liquid water or steam, when available, along with vaporized gasoline and air. The simulation was run under the following conditions and assumptions:

(a) The fuel processor is lit off in the catalytic partial oxidation mode (CPOX) at O/C = 1, when vaporized fuel is available and passes over a heated igniter coil.

(b) Liquid water can be fed to the nozzle without quenching the oxidation reactions once the ATR catalyst temperature exceeds 600 °C everywhere, starting at a rate corresponding to a S/C of 0.5. This ratio is maintained until the temperature of the reformate leaving the recuperator (HE1) exceeds 60 °C, at which point the water feed is gradually increased to S/C = 1. This constraint on feed water is imposed to limit condensation within the recuperator.

(c) A simple control algorithm is used to dynamically adjust the flow rate of air (O/C) to the ATR. The algorithm gradually raises or lowers O/C in an attempt to maintain the ATR at 775 ± 25 °C.

(d) The S/C ratio is gradually increased to the design point value of 2 after the heat exchangers (HE2–HE6) are heated and are able to generate steam for the ATR.

(e) The thermal mass of the catalytic reactors that are heated during the start-up time is 110% of the mass of the catalyst and the catalyst support. The 110% represents a combination of part of the supported catalyst and neighboring hardware, such as the containment walls, insulation, instrumentation, etc.

(f) With the possible assist of an ignition source, hydrogen can be oxidized on the shift catalyst even at room temperature and in the presence of >10% CO. The PrOx catalyst is assumed to be active at room temperature.

(g) A simple on–off control is employed to regulate the flow of oxidation air to the shift and PrOx reactors during start up. The flow of air to a catalytic reactor is momentarily shut off if the peak temperature exceeds the allowable temperature, chosen as 450/450/400/400 °C for the first/second/third/fourth stages of the shift reactor and 250/200/150 °C for the first/second/third stages of the PrOx reactor.

(h) The process water bypasses a heat exchanger (HE2–HE6) if the reformate temperature at the inlet of the downstream catalytic reactor is below the design temperature.

(i) The process water bypasses the high-temperature recuperator (HE1) if the quality of steam raised in the other heat exchangers (HE2–HE6) is less than one. If the steam is superheated, it is mixed with process air and the mixture flows through the coolant passages of the recuperator before entering the nozzle.

(j) For the purpose of this simulation, the air injections into the shift (WGS) reactors are terminated at 45 s. For the initial 45 s, the air feed rates into the PrOx reactors are set to the lesser of the two rates as determined by: (1) the gap between the actual and design temperature and (2) the inlet CO concentration and the stage stoichiometry. After 45 s, the air rates to the PrOx zones are determined only by the CO levels.

Fig. 4 shows the reformer operating in the CPOX mode (O/C = 1) for the first 5 s, by which time the ATR temperatures (Fig. 5) are found to have stabilized. The control algorithm

rapidly raises the O/C ratio to about 1.1 as the reforming mode transitions to ATR, as shown in Fig. 4. Over the next 25 s, the S/C is held at 0.5, and, as the recuperator heats up and elevates the preheat temperature of the air entering the ATR, the O/C is steadily reduced to below 0.9. At $t = 30$ s, the reformate temperature at the exit of recuperator reaches 60 °C (not shown). At this time, the control algorithm raises the S/C to 1 and dynamically adjusts the O/C to maintain the ATR exit at 775 ± 25 °C. According to this simulation, steam first becomes available (not shown) at about 45 s, at which point the S/C is rapidly increased to 2 and the O/C is adjusted to maintain the ATR temperature. The reformate leaving the ATR contains up to 24% CO in the CPOX mode, 15% CO at S/C = 0.5, 12% CO at S/C = 1 and <10% CO at S/C = 2.

Fig. 6 shows the calculated temperature profiles in the shift reactors. It is seen that it takes 30 s to heat the first and second stages above 350 °C and 45 s to heat the third stage above 300 °C. At the end of the start-up period of 45 s, only 60% of the fourth stage is above 300 °C.

Fig. 7 shows the calculated temperature profiles in the PrOx reactors. It indicates that within 30 s the first and second stages are heated above ~150 °C and the third stage is above 100 °C.

The simulated hydrogen yield from the fuel processor is plotted in Fig. 8 as a percentage of the rated design capacity. During the start-up period, it is desirable to oxidize all of the hydrogen produced in the ATR within the fuel processor to accelerate the heating of the catalytic reactors and the foam heat exchangers (HE2–HE6). This simulation indicates that it may not be possible to achieve 100% hydrogen utilization without producing hot zones in the reactors. Also, the hydrogen yield is below 90% (as a percentage of the FP capacity) until superheated steam is available and S/C >1.8. Thus, for faster start up, the nozzle has to be able to handle liquid water in quantities greater than S/C = 1.8. The effects of water on the reaction chemistry and the hydrogen yield are evident at 30 and 45 s, when the steam-to-carbon ratios (see Fig. 4) are changed.
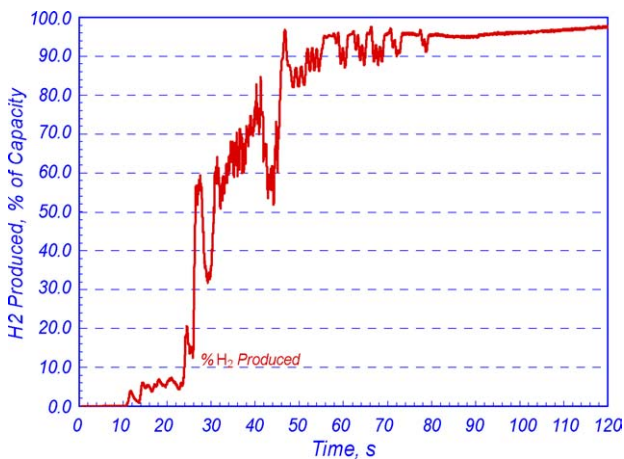

Fig. 8. Simulated hydrogen yield (as a percentage of rated capacity) from the fuel processor.

5. Three-dimensional CFD simulation used to meet design point conditions

The design and control strategy to meet the efficiency goals requires maintaining catalyst component temperatures very close to the design point temperatures given in Table 1. Variations in temperature and reactant mixture ratios are both temporal and spatial. The control system uses from one to three thermocouple point measurements to adjust feed rates to maintain conditions near the design operating point. Three-dimensional computational fluid dynamics (CFD) simulations for all major reactor components and the upstream reactant injection and mixing zones were used to determine or modify component designs, to provide a sufficiently uniform mixture over component cross-sections. Mixing zone designs optimized to meet uniformity constraints ensure that control based on point measurements keeps the entire cross-section of the reactor within a given tolerance value of deviation from the design operating point.

Minimization of the root mean square (rms) deviation of temperature, species concentration or mixture ratios as fluid enters catalyst reactor zones is necessary to achieve operation close to theoretical efficiency. Minimizing flow variable deviations is limited in practice by a variety of fabrication requirements, such as the need for retainer rings and the presence of tubing in the flow path. Limiting the maximum deviation from the mean is also a constraint in catalyst reaction zones, because local hot spots may degrade and shorten catalyst life. For example, the control system shuts off air to shift reactors WGS1 or WGS2 if a peak temperature of 450 °C is exceeded. In Fig. 6, WGS1 and WGS2 are operating near this peak temperature after 20 s. A 10% local deviation in O_2 concentration above the mean results in ~25 °C increase in adiabatic temperature rise in the shift reactors, which would cause a local hot spot of ~475 °C that would not be detected by the control system if it was not at a thermocouple position.

Three-dimensional CFD simulation was used to obtain component designs with O_2 concentration nonuniformities well under 10% at reactor stage inlet planes. To provide an additional flow path length for mixing air, injection points were placed upstream of heat exchangers HE2–HE6, as shown in Figs. 2 and 3. Depending on the alignment of air injectors with slots in the inlet planes of HE2–HE6, air mixing during flow through these heat exchangers reduces the O_2 concentration deviation by a factor between two and greater than 10 (Fig. 9). Because fabrication procedures could not guarantee the alignment required to maintain O_2 concentration deviations under 10%, an additional mixer component was inserted before the heat exchangers. The mixing performance of this additional mixer component is also plotted in Fig. 9 and was found to be acceptable for this project. Air injection upstream of HE1 was not feasible. For this case, a microchannel interleaved air injector was used at the HE1 outlet, with an additional mixer component just upstream of the WGS1 inlet.
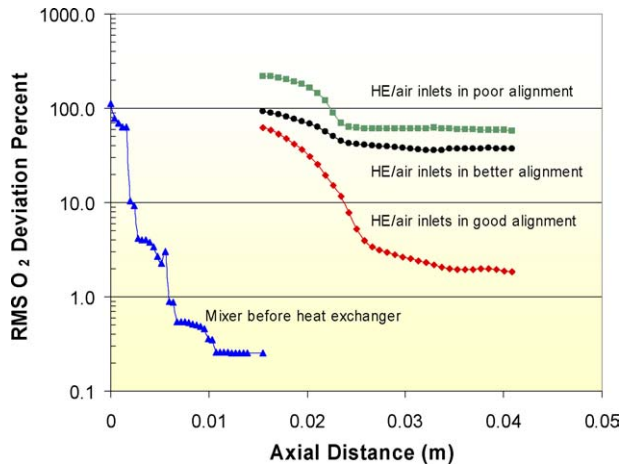
Fig. 9. CFD-calculated axial profiles of cross-section percent O_2 root mean square (rms) deviation through HE2 for good and poor alignment between air inlets and HE slots, compared to profile through a mixer added before HE2.

6. The fabricated fuel processor

The fuel processor layout (Fig. 10) is based on a series of concentric cylinders with the central cylinder containing the ATR zone and the first heat exchanger, HE1. Thereafter, the reformate flows through two annular paths that contain four WGS zones, five heat exchangers and three PrOx zones. The catalysts for the ATR and the four water–gas shift reactors are supported on a Microlith™ structure fabricated by Precision Combustion Inc. HE1, a microchannel heat exchanger fabricated by Pacific Northwest National Laboratory, is designed
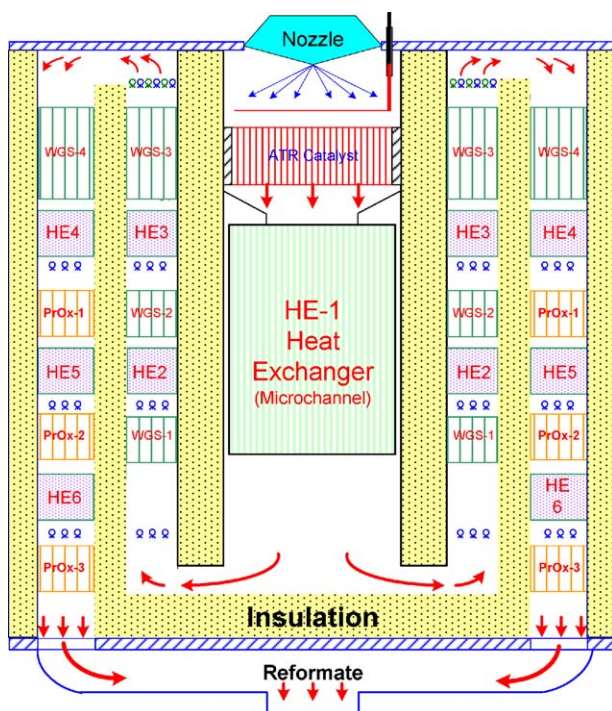
Table 2
Weights of the experimental fuel processor components

Component	Weight (g)	%
HE1 + air injection assembly	3140	14.8
HE2	898	4.2
HE3	898	4.2
HE4	1500	7.1
HE5	1500	7.1
HE6	1500	7.1
ATR assembly	578	2.7
WGS1	1276	6.0
WGS2	1460	6.9
WGS3	2163	10.2
WGS4	3978	18.7
P1	796	3.7
P2	791	3.7
P3	791	3.7
Total major components	21270	100

for a heat duty of 360 kW and an approach temperature of 100 °C. HE2–HE6 are carbon foam heat exchangers designed and fabricated by Oak Ridge National Laboratory. The three PrOx reactors use ceramic foam supports, and were designed and fabricated by Los Alamos National Laboratory.

ArvinMeritor Inc. fabricated the integrated fuel processor. The components were delivered to ArvinMeritor Inc. as stand-alone units. For mechanical integrity during transport and ease of welding and assembly, no attempt was made to reduce the thickness of walls and other support structures. Multiple thermocouples and sampling ports were built into some of the structures, as received. Additional thermocouples, pressure taps, sampling ports, air and water injection ports, mixing zones, pressure relief vents, etc., were installed between the components, as needed.

Table 2 lists the weights of the major components of the fuel processor, as received. The right column indicates the percentage contribution of each of the major components. Not surprisingly, the fourth stage of the water–gas shift reactor (WGS4) was the heaviest component, accounting for 18.7% of the total weight of the major components. The fuel processor was weighed at various times during the assembly process. The central cylinder, the inner annulus and the outer annulus weighed 11.8, 21.8 and 42.2 kg, respectively, totaling 76 kg for the fuel processor hardware.

The fuel processor can operate at its maximum design point efficiency only after it reaches its normal operating temperature profile. Warming up the fuel processor to this state requires an amount of fuel energy that is determined by the thermal mass (mass times the heat capacity) and the required temperature rise of the various components. Fig. 11 shows the distribution of the mass and the fuel energy required for the major components. It was estimated that heating up the major components of the experimental FP would require a minimum of 2.9 MJ of fuel energy. This is equivalent to 0.025 gal or 95 mL, of gasoline. The high-temperature heat exchanger, HE1, requires more fuel energy (~27%) than the heaviest component, WGS4, which needs ~19%. The WGS4 con-
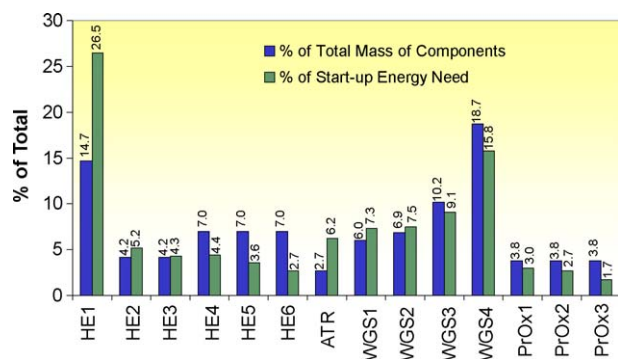

Fig. 10. Layout of fuel processor components.

Fig. 11. Distribution of mass and energy needs for start up of the fuel processor.

verts only 6.9% of the total CO converted in the shift reaction zones, but contributes 45% to the mass of the shift reactor zones. These figures suggest that eliminating the fourth water–gas shift zone(s) and reducing the mass of the heat exchangers, especially those at high temperature, offer the best potential for reducing the start-up fuel energy consumption, albeit with possibly a small reduction in steady-state fuel processor efficiency.

7. Conclusions

A fuel processor has been designed along with a parallel heating start-up strategy. The design is based on catalytic ATR/WGS/PrOx zones separated by temperature-control zones that use microchannel and foam heat exchangers. Simulation shows that the fuel processor can deliver 90% of the rated hydrogen capacity within 60 s. Based on the mass of the delivered components, it is estimated that the 10-kW$_e$ laboratory unit will require 2.9 MJ of gasoline to reach the design point temperatures. The high-temperature heat exchanger (HE1) and the low-temperature shift zone (WGS4) represent the largest contribution to this start-up fuel consumption.

Acknowledgments

Appendix A

The U.S. Department of Energy's technical targets for an on-board fuel processor. *Source*: Multi-Year Research, Development and Demonstration Plan Planned Activities for 2003–2010 (Draft 6/3/03) [http://www.eere.energy.gov/hydrogenandfuelcells/mypp].

Technical targets: fuel-flexible fuel processors[a] to generate hydrogen-containing fuel gas from reformulated gasoline containing 30 ppm sulfur, average for 50-kW$_e$ (net) fuel cell systems[b]

Characteristics	Calendar year		
	2003 Status	2005	2010
Energy efficiency[c] (%)	78	78	80
Power density (W L^{-1})	700	700	800
Specific power (W kg^{-1})	600	700	800
Cost[d] ($ per kW$_e$)	65	25	10
Cold start-up time to maximum power			
@ −20 °C ambient temperature (min)	TBD	2.0	1.0
@ +20 °C ambient temperature (min)	<10	<1	<0.5
Transient response (time for 10–90% power) (s)	15	5	1
Emissions[e]	<Tier 2 Bin 5	<Tier 2 Bin 5	<Tier 2 Bin 5
Durability[f] (h)	2000[g]	4000[h]	5000[i]
Survivability[j]	TBD	−30	−40
CO content in product stream[k]			
Steady-state (ppm)	10	10	10
Transient (ppm)	100	100	100
H$_2$S content in product stream (ppb)	<200	<50	<10
NH$_3$ content in product stream (ppm)	<10	<0.5	<0.1

[a] With catalyst system suitable for use in vehicles.

[b] Excludes fuel storage; includes controls, shift reactors, CO cleanup, heat exchangers. All targets must be achieved simultaneously and are consistent with those of FreedomCAR.

[c] Fuel processor efficiency = total fuel cell system efficiency/fuel cell stack system efficiency, where total fuel cell system efficiency accounts for thermal integration. For purposes of testing fuel-processor-only systems, the efficiency can be estimated by measuring the derated heating value efficiency (lower heating value of H$_2$ × 0.95/lower heating value of the fuel in) where the derating factor represents parasitic system power losses attributable to the fuel processor.

[d] High-volume production: 500,000 units per year.

[e] 0.07 g mile^{-1} NO$_x$ and 0.01 g mile^{-1} PM (particulate matter).

[f] Time between catalyst and major component replacement; performance targets must be achieved at the end of the durability period.

[g] Continuous operation.

[h] Includes thermal cycling.

[i] Includes thermal and realistic driving cycles.

[j] Performance targets must be achieved at the end of an 8-h cold soak at specified temperature.

[k] Dependent on stack development (CO tolerance) progress.

References

[1] http://www.eere.energy.gov/hydrogenandfuelcells/annual_report04.html.
[2] Fuel Cells Bulletin (6) June 2003.
[3] S. Ahmed, M. Krumpelt, Int. J. Hydrogen Energy 24 (4) (2001) 291–301.
[4] S. Ahmed, Presented at the 2003 DOE Hydrogen and Fuel Cells Merit Review Meeting, May, 2003.
[5] S. Springmann, M. Bohnet, A. Docter, A. Lamm, G. Eigenberger, J Power Sources 128 (2004) 13–24.